# Oxidation Behavior of Ni in Molten Carbonate

**Naobumi Motohira,* Takahiro Takai, Nobuyuki Kamiya, and Ken-ichiro Ota**

Department of Energy & Safety Engineering, Yokohama National University,
79-5 Tokiwadai, Hodogaya-ku, Yokohama 240-8501

(Received November 12, 1998)

The oxidation behavior of Ni in molten carbonate was evaluated by chronopotentiometry. The oxidation of Ni in molten carbonate proceeded in a two-step reaction. The first step of oxidation was independent of the specimens' nature and depended on $P_{CO_2}$. On the other hand, the second step of oxidation depended on the batch of the specimens, and was independent of $P_{CO_2}$. The corrosion product in both oxidation processes was divalent Ni oxide, namely NiO.

A molten carbonate fuel cell (MCFC) has advantages from the point of a high-efficiency power-generation system. One of the most serious problems for the commercialization of MCFC is corrosion of structural materials, which causes electrolyte loss, and subsequently leads to an increase of the reaction resistance. The corrosion behavior of Ni, which is one of the main elements of MCFC's components in molten carbonate, has been reported by many researchers.[1—9] Janz et al.[1,2] reported that anodic polarization curves showed the characteristic feature of passivation, but that Ni was severely corroded because of imperfect protection by the corrosion product of NiO scale. Nishikata et al.[3,4] reported two peaks on the anodic polarization curves for a Ni electrode in molten carbonate. They insisted that those two peaks corresponded according to the following two reactions:

$$Ni + O^{2-} = NiO + 2e^{-}, \quad (1)$$

$$Ni + CO_3^{2-} = NiO + CO_2 + 2e^{-}. \quad (2)$$

They suggested that the buffer capacity of reaction (3) is weak because of the fact that these two reactions can be clearly distinguished:

$$CO_3^{2-} = CO_2 + O^{2-}. \quad (3)$$

Nishina et al.[5,6] measured the time dependence of the open-circuit potential (OCP) for a Ni electrode in molten carbonate. They found two potential plateau in OCP, and insist that the first plateau represents the oxidation of $Ni^{2+}$ to $Ni^{3+}$ and the second plateau corresponds to the rest potential of the oxygen electrode. Tomczyk et al.[7] reported on the electrochemical behavior of a Ni electrode in molten Li/K and Na/K carbonate, and suggested that the plateau observed at ca. −0.35 V would be associated with the incorporation of Li from Li/K carbonate into the NiO lattice.

In this study, the oxidation behavior of a Ni electrode in molten carbonate was evaluated by chronopotentiometry so as to reveal the oxidation process of Ni in molten carbonate.

## Experimental

$Li_2CO_3$ and $K_2CO_3$ were used as the electrolyte in this study. The composition of molten carbonate was the general composition of MCFC cells; Li : K = 62 : 38 eutectic composition, whose melting point was 761 K. The carbonate reagent was purified by the following process. Each carbonate reagent (100 g in total) was weighed and mixed in a dry box filled with nitrogen gas so as to prevent moisture. Mixed carbonate reagents were dried in a vacuum at 298 K for 30 min, then at 373 K for 30 min, and finally at 623 K for 12 h. Dried carbonates were treated under a pure $CO_2$ atmosphere at 1023 K for 24 h with $CO_2$ bubbling in order to remove any remaining moisture. Then, the temperature of the carbonate melt was down to 923 K and the atmosphere was controlled based on the experimental condition; $P_{CO_2} = 10^{-4}$ to 1 atm balanced by Ar to be a total pressure of 1 atm, and a gas-flow rate of 50 ml $min^{-1}$. Crashed NiO pellets were soaked in molten carbonate so that the concentration of Ni ion could be saturated under each condition.

1.5 mm$\phi$ of Ni wire (99.7% purity) was used as the working electrode, which had an electrode area of 0.5 $cm^2$. 2 mm$\phi$ of gold wire was used for the counter and reference electrodes. The oxygen electrode with an atmosphere of $O_2 : CO_2 = 2 : 1$ was adopted as the reference electrode.

The chronopotentiometry method was achieved at a current of 1 to 120 mA, and measured until the potential of the rest potential of the oxygen electrode. For a comparison, a potential sweep was also measured. The result was recorded by an $x$–$y$ recorder while a transient memory was used when the reaction time of the first transient was too short. After the experiment, the cross-sectional image of the specimens were observed by SEM and the corrosion products were identified by an X-ray diffraction analysis. The current efficiency was estimated by measuring the amount of weight loss for each electrode, by removing corrosion products with acetic acid.

## Results and Discussion

Figure 1 shows the polarization curve for a potential-sweep measurement under $CO_2$ 1 atm atmosphere. Potential was swept from −0.8 to 0 V vs. standard oxygen electrode at a rate of 0.1 to 5 mV $s^{-1}$. Two peaks were clearly observed at around −0.6 and −0.4 V, which was a similar behavior

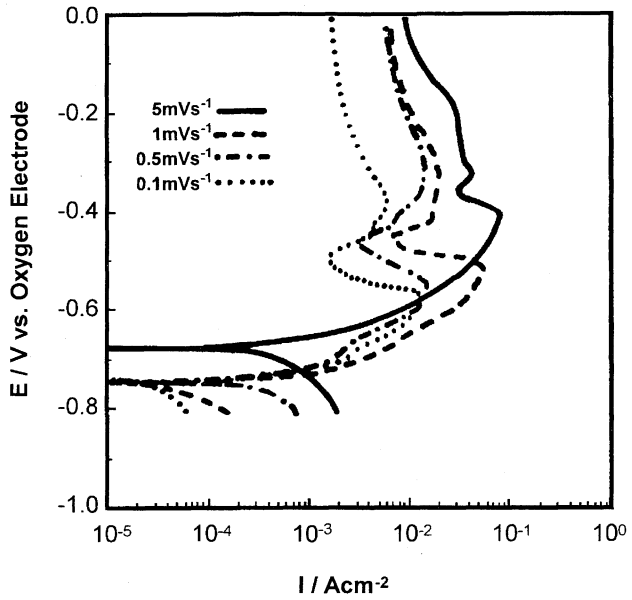


Fig. 1. Sweep rate dependence of polarization curves for the corrosion of Ni in molten carbonate at 923 K.

to that reported by other authers.[8] The typical chronopotentiogram is shown in Fig. 2. Two transition periods were obviously found in the figure. These two potential plateaus corresponded to the peak potential in the potential-sweep method.

The electrode after the first transition period showed a color of light green, which suggested the formation of NiO on the surface, but turned black after the second transition period. If the oxidized nickel was assumed to be divalent, the current efficiency calculated from the weight loss should be as shown in Table 1. The current efficiency was nearly 100% at both the first and second transition periods, which insisted that all the electrode reactions were Ni oxidization and that

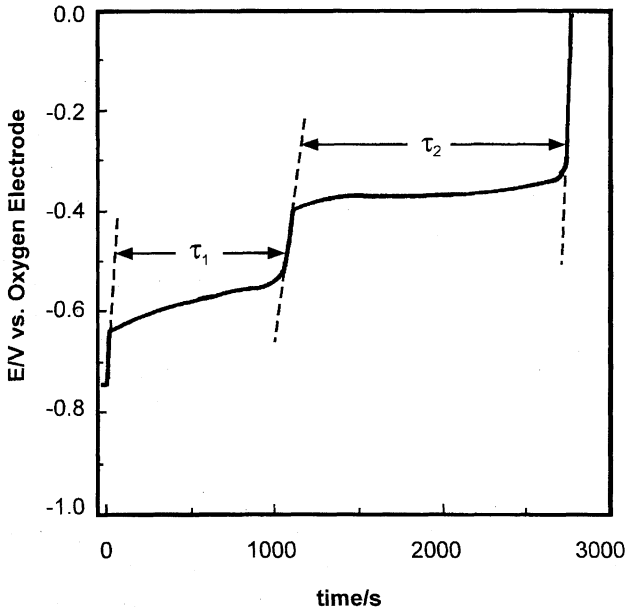


Fig. 2. Typical chronopotentiogram for the corrosion of Ni in molten carbonate.

Table 1. Current Efficiency of Ni Corrosion in Molten Carbonate

| Condition ($P_{co_2}$=1 atm) | | $\Delta W$/g | $Q$/C cm$^{-2}$ | $\varepsilon$/% |
|---|---|---|---|---|
| ~ end of $\tau_1$ | 873 K<br>10.1 mA cm$^{-2}$ | 13.50 ×10$^{-3}$ | 87.1 | 103 |
| | 923 K<br>19.7 mA cm$^{-2}$ | 5.50 ×10$^{-3}$ | 38.6 | 92.4 |
| ~ end of $\tau_2$ | 873 K<br>9.73 mA cm$^{-2}$ | 21.54 ×10$^{-3}$ | 133.1 | 103 |
| | 873 K<br>9.96 mA cm$^{-2}$ | 18.31 ×10$^{-3}$ | 111.3 | 108 |
| | 923 K<br>9.92 mA cm$^{-2}$ | 7.89 ×10$^{-3}$ | 58.2 | 88.4 |
| | 973 K<br>9.92 mA cm$^{-2}$ | 4.49 ×10$^{-3}$ | 25.6 | 114 |

divalent nickel was formed at both the first and second transition periods. The X-ray diffraction analysis confirmed that only NiO existed. This suggests that the formation of trivalent nickel was not the main corrosion reaction in molten carbonate. Specimens were washed by acetic acid after the experiment to remove the oxide scale. The scale formed after the first transition period was easily dissolved, while that of the second transition period was difficult to remove. The oxide scale formed in the first transition period was considered to be changed to a tight scale after the second transition period.

The cross-sectional SEM image for the electrode picked up after the first transition period is shown in Fig. 3. The electrode was oxidized at 873 K in $CO_2$ at 1 atm and a current density of 10 mA cm$^{-2}$. The thickness of the oxide scale was about 34 μm. The thickness of NiO scale was estimated to be 40 μm from a electricity of 76.1 C cm$^{-2}$ during 7750 s of the experiment, which was comparable to the measured value. A needle-like oxide scale was grown perpendicular to the surface, and was found to be porous.

Figure 4 shows the cross-sectional SEM image after the second transition period under the same condition as in Fig. 3. A double-layered oxide scale was obviously observed. The

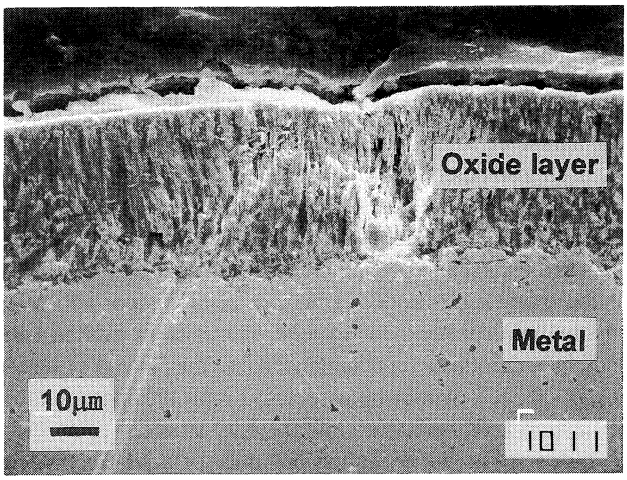


Fig. 3. Cross sectional photograph for Ni electrode after the first transition.

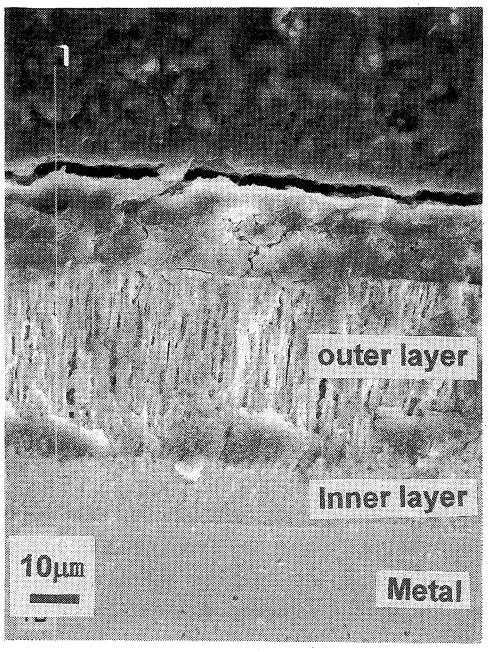


Fig. 4. Cross sectional photograph for Ni electrode after second transition.

thickness of the outer scale was 39 μm, and calculated thickness of the first transition period was 42 μm based on the electric quantity of 81.1 C cm$^{-2}$. The thickness of the inner scale was 11 μm, and the calculated value of the second transition period was 17 μm from a electric quantity of 33.5 C cm$^{-2}$. The observed and calculated thickness were in fairly good correspondence, which suggests that the outer and inner scales were also NiO, while the outer scale was formed during the first transition period and the inner scale was formed during the second transition period.

Table 2 gives the transition period for different batches of Ni wire. Each Ni was 99.7% in purity and 1.5 mm$\phi$ in diameter. The experimental condition was 923 K under $CO_2$ at 1 atm and a current density of 20 mA cm$^{-2}$. Table 2 indicates that the first transition period was independent of the batches, while the second transition period differed at least five times. The reaction which occurred in the second transition period depended on the batches, which suggests that some reaction in solid phase was responsible for the transition period. The batch of Ni(A) was used for the following experiments in order to avoid any difference in the transition period among the specimens.

Figure 5 shows the dependence of the logarithmic current density and the potential at the quarter point of each transition period ($E_{\tau/4}$). Each curve obeyed Tafel's law, and the slope was about 100 mV/decade, indicating that the rate-determining step was the charge-transfer process at 1/4 of the

Table 2. Sample Dependence of Transition Time at the Current Density of 20 mA cm$^{-2}$ in 1 atm $CO_2$ at 923 K

| Specimens | $\tau_1$ / s | $\tau_2$ / s |
|---|---|---|
| Ni(A) | $1.49 \times 10^3$ | $1.03 \times 10^3$ |
| Ni(B) | $1.43 \times 10^3$ | $5.43 \times 10^3$ |

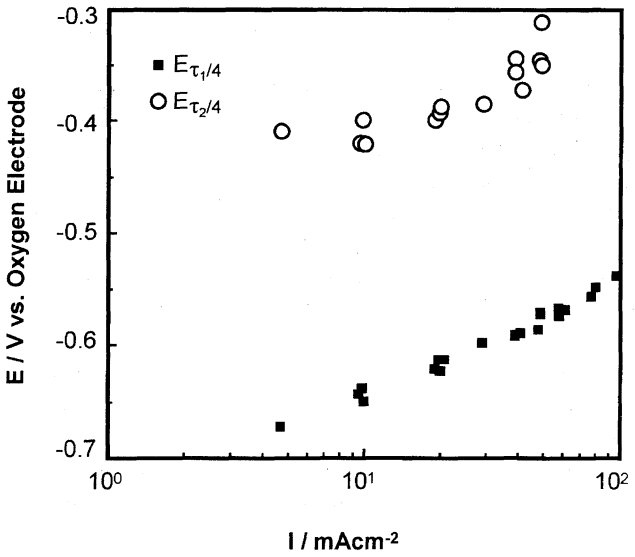


Fig. 5. *I–E* curve of Ni corrosion in molten carbonate.

transition period. The potential curve of the second transition period apparently shows diffusion limiting current density of about 50 mA cm$^{-2}$.

Figure 6 shows the relationship between the current density and each transition period. The figure shows that each transition period decreases when the current density increases. The slope of each curve was about $-2$, and the second transition period rapidly diminished at a higher current density, because of the limiting current density observed in Fig. 5.

The reaction rate at the surface was constant in the chronopotentiometry because of the constant current density,

$$\frac{dx}{dt} \approx \frac{dQ}{dt} = i = \text{const.} \tag{4}$$

Assuming that the diffusion rate of the reacting species in oxide was determined by the potential slope in the oxide scale, the diffusion rate should be inversely proportional to the thickness of oxide scale,

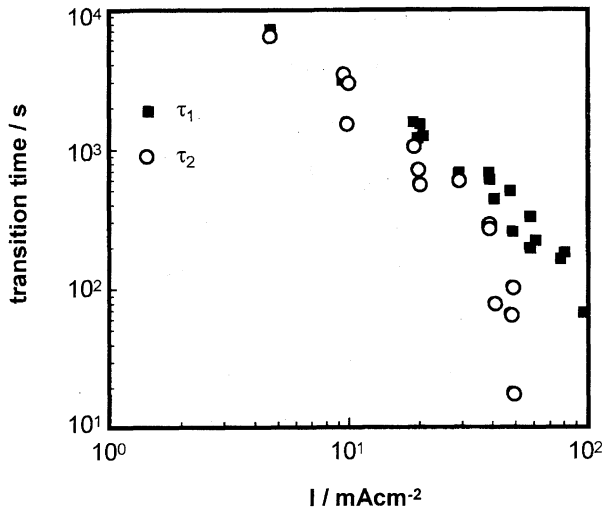


Fig. 6. Relationship between current and $\tau$ of NiO formation in molten carbonate.

$$\frac{dx}{dt} = \frac{k}{x}. \tag{5}$$

At first, the volume diffusion rate was larger than surface-reaction rate (surface-reaction rate < volume-diffusion rate). The concentration gradient of the reactant in the oxide scale decreased in accordance with the growth of the oxide scale. Then, the volume-diffusion rate became equivalent to the surface-reaction rate at the end of the transition period (surface-reaction rate = volume-diffusion rate). After the transition period, the diffusion of a reactant could not follow up the rate of surface reaction (surface-reaction rate > volume-diffusion rate). Then, the potential would jump to another potential at $\tau$. Thus, the current density of an experiment corresponds to the critical surface-reaction rate at the transition time. Figure 7 shows a schematic drawing for the above discussion.

From Eqs. 4 and 5, the following equation is introduced:

$$i = \frac{k}{Q} = \frac{k}{i\tau}. \tag{6}$$

Thus, the product of $\tau$ and the square of current density is constant,

$$i^2\tau = k = \text{const.} \tag{7}$$

The amount of electric quantity flowed during the transition period ($\tau$) is expressed by $Q = i\tau$; thus, Eq. 7 is transformed to

$$Q^2 = k\tau. \tag{8}$$

Considering that the total electric quantity is directly related to the thickness of the oxide scale, Eq. 8 was treated like the parabolic law in the case of the high-temperature corrosion of metals,

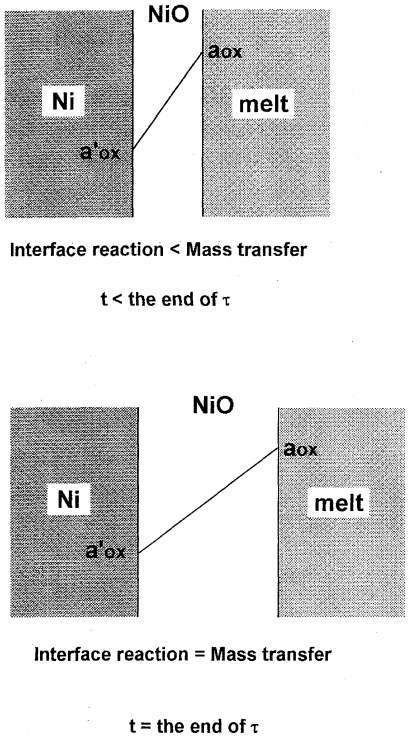


Fig. 7. Schematic diagram for transition time determining process. $a_{ox}$ : activity of oxidant.

$$x^2 = k't. \tag{9}$$

Then, the transition period ($\tau$) should depend on the volume-diffusion rate in the oxide scale.

Based on the above point of view, the rate-determining step before the transition period should be the charge transfer-reaction, which was consistent with the fact that *I–E* curves obeyed Tafel's law. Considering that the slope of the $\log(\tau)$–$\log(I)$ curves in Fig. 6 was $-2$, the following relations were obtained,

$$\log \tau = A - 2\log i, \tag{10}$$

$$i^2\tau = 10^A. \tag{11}$$

Equation 11 is the same as Eq. 7, which supports the above discussion.

In the case of a higher current density, where diffusion-limiting current density was observed in the second transition period, as in Fig. 5, the diffusion rate in the oxide scale would be less than the surface-reaction rate (surface reaction rate > volume diffusion rate). This should be the reason why a diffusion-limiting current was observed in the second transition period.

Figure 8 shows the $P_{CO_2}$ dependence of each transition time for a current density of 20 mA cm$^{-2}$ at 923 K. The transition time became longer in accordance with the increase of $P_{CO_2}$ in the first transition time, while the second transition time was independent of $P_{CO_2}$. This result suggested that $P_{CO_2}$ affected the activity of the reaction species during the first transition period. However, reaction (12) should not be the anode reaction in this case, because no electrons were transferred to an electrode:

$$Ni + CO_2 \rightarrow NiO + CO. \tag{12}$$

In molten carbonate, the activity of $CO_2$ and $O^{2-}$ are inversely proportional in accordance with equilibrium (3). If the change of $P_{CO_2}$ directly affected $a_{O^{2-}}$, the anode reaction

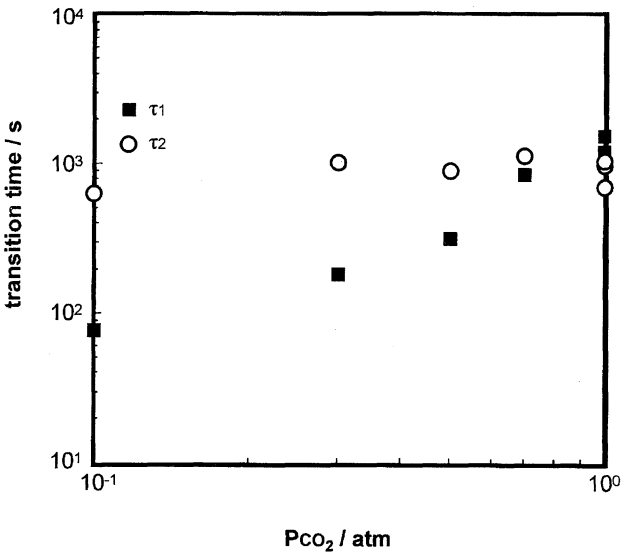


Fig. 8. Relationship between $P_{CO_2}$ and $\tau$ for NiO formation in molten carbonate.

would be the following reaction:

$$Ni + O^{2-} = NiO + 2e^{-}, \quad (1)$$

On the other hand, the reaction in the second transition period was independent of $P_{CO_2}$, which indicated that the activity of the reaction species in the second transition was not affected by $P_{CO_2}$. Thus, the reaction in the second transition period would be

$$Ni + CO_3^{2-} = NiO + CO_2 + 2e^{-}. \quad (2)$$

Reaction (2) is a $CO_2$ gas-evolution reaction at the same time, which is consistent with reported results.[3,9]

## Conclusion

Chronopotentiometry was performed for a Ni electrode in molten carbonate. Two steps of the rest potential were observed, which corresponded to the two peaks observed in a potential-sweep measurement. The first transition period became longer in proportion to the increase in $P_{CO_2}$, the reaction of which would be related to the activity of $O^{2-}$ in molten carbonate. The reaction in the second transition period was independent of $P_{CO_2}$, and the transition period depended on a sample's nature.

This study was supported by International Joint Research Grants from the New Energy and Industrial Technology Development Organization (NEDO) of Japan. A part of this study was also supported by a Grand-in-Aid for Scientific Research No. 09750899 from the Ministry of Education, Science, Sports and Culture.

## References

1) G. J. Janz and A. Conte, *Electrochem. Acta*, **9**, 1269 (1964).
2) G. J. Janz and A. Conte, *Electrochem. Acta*, **9**, 1279 (1964).
3) A. Nishikata and S. Haruyama, *J. Jpn. Inst. Metals*, **48**, 720 (1984).
4) A. Nishikata and S. Haruyama, *Corrosion*, **42**, 578 (1988).
5) T. Nishina, K. Takizawa, and I. Uchida, *J. Electroanal. Chem.*, **263**, 87 (1989).
6) K. Takizawa, T. Nishina, and I. Uchida, *Denkikagaku*, **58**, 442 (1990).
7) P. Tomczyk, H. Sato, K. Yamada, T. Nishina, and I. Uchida, *J. Electroanal. Chem.*, **391**, 125 (1995).
8) O. F. Devereux, K. Y. Kim, and K. S. Yeum, *Corros. Sci.*, **23**, 205 (1983).
9) J. R. Selman, "Proc. on the 2nd International Fuel Cell Conference," Feb. 5-8, Kobe, Japan, Abstr., pp. 103—110 (1996).